Emission and Transport of Carbonaceous Aerosols in Urbanized Coastal Areas in China

Bing Chen[1,2], Ke Du[1*], Yang Wang[1], Jinsheng Chen[1*], Jinping Zhao[1], Kai Wang[1], Fuwang Zhang[1], Lingling Xu[1]

[1] *Key Lab of Urban Environment and Health, Institute of Urban Environment, Chinese Academy of Sciences, Xiamen, Fujian Province, 361021, China*
[2] *Associate Unit CSIC-University of Huelva "Atmospheric Pollution", University of Huelva, E21071 Huelva, Spain*

ABSTRACT

Elemental and organic carbon (EC and OC), the principal short-lived climate forcers, were measured in fine particulate matter ($PM_{2.5}$) collected at urban and rural sites in continental edge in Southern China. The carbonaceous matter (CM) contributed an average of $28.5 \pm 7.2\%$ (1 SD) of the mass of $PM_{2.5}$ in urban areas and $30.3 \pm 8.2\%$ in rural areas. The annual average OC concentrations in $PM_{2.5}$ in urban and rural areas were 7.6 ± 4.3 and 5.7 ± 3.1 μg/m^3, respectively; and the annual average EC concentrations were 2.4 ± 0.8 and 1.3 ± 0.7 μg/m^3, respectively. The higher EC concentration in urban area than in rural area showed significant anthropogenic emissions to the urban atmosphere. EC and OC concentrations displayed good correlation in samples collected in urban area during winter monsoon season, suggesting a dominant emission source (mostly traffic-related) in urban area. The carbonaceous aerosol pollution in the rural coastal receptor area can be attributed to the local emission and transport of air pollutants from urbanized areas in the eastern part of China. The surface observation together with backward trajectory analysis, satellite imaging, and meteorological simulation indicate that air pollutants transported from emission hotspots in the urbanized Eastern China area had caused an increase in the concentration of carbonaceous aerosols in the rural continental edge by a factor of 2–3. This significant aerosol forcing of the Chinese outflow plume should be paid attention in the study of air quality and climate changes in Eastern/Southern Asia.

Keywords: Elemental carbon; Organic carbon; $PM_{2.5}$; Urban emission; Dispersion.

INTRODUCTION

Elemental carbon (EC) has a graphite-like structure, which intensively absorbs solar radiation, and is probably the most significant agent of global warming after CO_2 with a climate forcing of 0.4–0.9 W/m^2, which is roughly one quarter to one half of the climate warming effect of CO_2 (Ramanathan and Carmichael, 2008; UNEP and WMO, 2011). The atmospheric EC causes a net global warming up to 0.8°C (Chung and Seinfeld, 2005; Chung *et al.*, 2005; Ramanathan and Carmichael, 2008). EC is emitted directly from combustion sources and undergoes little chemical transformation, which makes it a good indicator for primary anthropogenic air pollution (Xiao *et al.*, 2011; Kim *et al.*, 2011). Organic carbon (OC) is a mixture of hydrocarbons and oxygenate compounds, which constitutes the rest of the carbonaceous aerosols (Gu *et al.*, 2010). OC can be emitted directly in particulate form (primary) or formed in the atmosphere from semi- and low-volatile products of chemical reactions involving reactive organic gases (secondary). Moreover, carbonaceous aerosols play important roles in the reproduction of biological organisms and can cause or enhance diseases (Pöschl, 2005).

The atmospheric lifetimes of EC and OC are about one week (UNEP and WMO, 2011). These rapid atmospheric turnovers mean that reductions in emissions of carbonaceous aerosols would result in a quicker effect on the climate than from reduction strategies just focusing on CO_2, the key long-lived climate forcer (atmospheric lifetime of ~100 years). The major source categories of combustion-derived carbonaceous aerosols are fossil fuel (e.g., diesel traffic and coal for energy), and biomass combustion (e.g., wood and manure as fuel and agricultural crop residue burning) (Cao *et al.*, 2006; Ho *et al.*, 2006; Zhang *et al.*, 2009b). Emission inventory models suggest that the anthropogenic activities in China might account for 25% of global EC emissions (Zhang *et al.*, 2009a; Chow *et al.*, 2010). The Chinese EC emission exerts a particularly strong influence on the climate in Asia where it rivals CO_2. Secondary effects include worsen atmospheric brown clouds (UNEP and WMO, 2011), weakened Asian monsoons (Menon *et al.*, 2002),

---
* Corresponding author. Tel.: +86-592-6190767
  E-mail address: kdu@iue.ac.cn; jschen@iue.ac.cn

and melting of the Himalayan glaciers (Xu *et al*., 2009). Mitigation of Chinese emissions offers a possibility to slow down and delay the onset of dangerous anthropogenic interference with the air and climate system. However, emissions of carbonaceous aerosols increased by 14% during the last five years (Zhang *et al*., 2009a), and mitigation efforts are hampered by poor knowledge of emission sources and transport pattern.

It is suspected that urbanized areas of China significantly account for the emissions of carbonaceous aerosols (Avino *et al*., 2011; Shi *et al*., 2010). More than 70% of major cities and 40% of total population of China are located in coastal areas (Cao and Wong, 2007). Coastal development in China plays a leading role in the national economy, accounting for 60% of its industrial production and 55% of gross domestic product (GDP) (Wang, 1992; Cao and Wong, 2007). The industrialization and urbanization in coastal areas of China should be a great contribution to anthropogenic emissions. In this study, we measured EC and OC concentrations in fine particulate matter (PM$_{2.5}$, particles smaller than 2.5 μm in aerodynamic diameter) at urban and rural sites in Southern China continental edge. The aim is to characterize the emission and transport of carbonaceous aerosols in Eastern and Southeastern Asia.

METHODS

Research Sites

Xiamen, which is located in Southern China coastal area, is an ideal sampling site for intercepting Chinese continental outflow in southeastern pathway (Liu *et al*., 2003, Fig. 1(a)). The whole region has a southern subtropical monsoon climate, with an annual mean temperature of 20.8°C. During the winter monsoon season (winter and autumn), the northern airflow from inland China brings cold and dry air to Xiamen, whereas during the summer monsoon season (March to September), the southern airflow brings brisk wind and marine air mass. Annual precipitation is 1143.5 mm, 80% of which occurs from March to September.

The field sampling for PM$_{2.5}$ occurred at three urban sites (24°26'N, 118°5'E; 24°29'N, 118°6'E; 24°29'N, 118°2'E; 20 m high above ground level (AGL)) and two rural sites (24°37'N, 118°3'E, 20 m AGL; 24°49'N, 118°9'E, 10 m AGL) in Xiamen (Fig. 1(b)). Urban Xiamen situates on an island connecting East China Sea and South China Sea. The three urban sites were selected to cover the main roads/streets, downtown, and nearby residential areas. Meanwhile, west of the city is an industrial area including a coal-fired power plant. Potential emission sources nearby the sampling sites in the urban area thus included motor vehicles, industrial emissions, and residential homes. Rural areas in Xiamen stretch out along the Southern China coast, and mountain forest spreads over the north to west. The two rural sites (~20 and 40 km from urban Xiamen) have similar surrounding of water body, woods and a few farmlands. The rural sampling sites are considered to be under the influence from biogenic emission, biomass burning in a few local residences, soil dust particles from farmlands and local country roads.

Samples and Measurements

PM$_{2.5}$ was collected on quartz filters (90 mm, Whatman, Quartz Microfibre Filters, Kent, UK) mounted on a mid-volume atmospheric sampler at the flow-rate of 100 L/min for 12–48 h. The total air volumes through the sampler for each sample were between 72–288 m^3. A constant flow-rate within an uncertainty of ±3% was obtained during sampling periods. The atmospheric sampler (TH-150C-III, Wuhan Tianhong Instrument Co., Ltd, China) consists of a size selective inlet followed by impactors to obtain a cut efficiency of 2.5 ± 0.2 μm. Quartz filters were pre-combusted at 450°C for 4 h before sampling. The filters were weighed (0.1 mg accuracy) before and after sampling to determine the total mass of collected PM$_{2.5}$. Before weighting, the filters were dried in an electronic desiccator at 25°C and relative humidity of 50% for 24 h. Then the sample filters were stored in a refrigerator before analysis.

A total of 64 samples were collected at three urban and two rural sampling sites. A 2.0 cm^2 piece of filter was cut off from each sample and analyzed with an automated semi-continuous thermal-optical transmittance (TOT) carbon
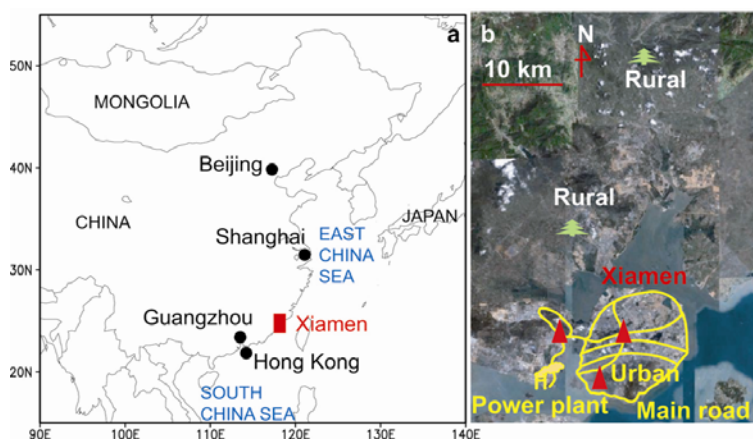

Fig. 1. Map (b) showing the sampling campaign at three urban (triangle) and two rural sties (tree-icon) in Xiamen in Southern China continental edge, together with (a) major megacites in the eastern part of China (Beijing, Shanghai, Guangzhou and Hong Kong).

analyzer (Sunset Laboratory, Inco, Portland, OR, USA) to determine the OC and EC loadings on that filter. TOT method for analysis of OC/EC follows the protocol specified by the National Institute for Occupational Safety and Health (NIOSH) (Birch and Cary, 1996; NIOSH, 1999). Detailed principle of Sunset analyzer determining OC and EC concentrations was described in the literature (Yang and Yu, 2002; Lim *et al*., 2003; Bae *et al*., 2004; Jeong *et al*. 2004; Rice, 2004; Arhami *et al*., 2005; Bauer *et al*., 2009). Replicate analyses of sucrose standard and filter samples showed an uncertainty of ~10% for OC and EC measurements. The concentrations of OC, EC, and $PM_{2.5}$ were reported as mass in a unit volume of air ($\mu g/m^3$). Carbonaceous matter (CM) was estimated from

$$CM = k \times OC + EC \qquad (1)$$

where "k" applied the values of 1.6 and 2.1 for urban and rural aerosols, respectively (Turpin and Lim, 2001).

RESULTS AND DISCUSSION

Daily Levels of EC and OC in $PM_{2.5}$

Fig. 2 shows the observed concentration of EC and OC in $PM_{2.5}$ in urban and rural areas of Xiamen. The EC concentrations in urban area were in the range of 1.4 to 4.9 $\mu g/m^3$, giving an annual average of 2.4 ± 0.8 $\mu g/m^3$ (1 SD). The EC concentrations in rural area were in the range of 0.4 to 2.8 $\mu g/m^3$ (average 1.3 ± 0.7 $\mu g/m^3$), which were lower than those values in urban area by a factor of 2. OC concentrations for $PM_{2.5}$ in urban area varied from 1.6 to 15.5 $\mu g/m^3$. The OC levels in rural area varied from 1.7 to 13.6 $\mu g/m^3$, which showed no significant difference from the values in urban area (student t-test at the level of significance of 5%).

It was noted that the observed mean-$PM_{2.5}$ of 53.4 ± 25.0 $\mu g/m^3$ in Xiamen, although not representative for the annual mean due to the limited coverage, exceeded the United States' National Ambient Air Quality Standard (NAAQS, http://
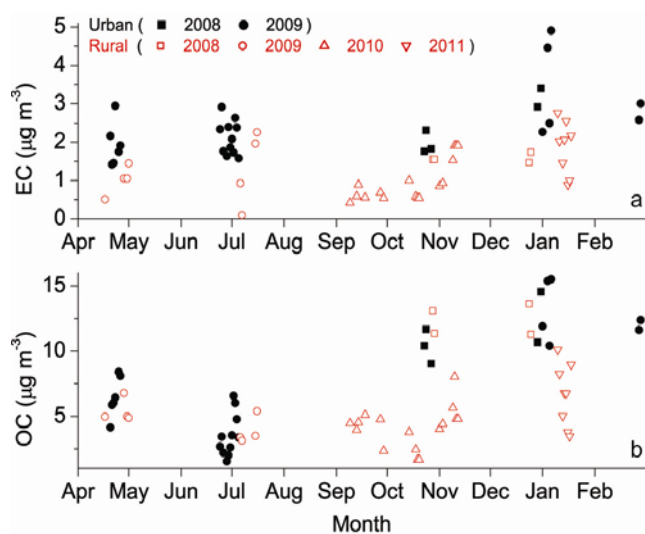
www.epa.gov/air/particlepollution/standards.html) of annual-mean 15 $\mu g/m^3$ for $PM_{2.5}$. Fig. 3 shows the relationships between $PM_{2.5}$ and carbonaceous aerosol concentrations. CM made the contributions of 28.5 ± 7.2% and 30.3 ± 8.2% to $PM_{2.5}$ (CM/$PM_{2.5}$) in urban and rural areas, respectively. The relatively high value of CM/$PM_{2.5}$ in rural area indicated probably significant contribution of biogenic organic aerosols (e.g., secondary organic carbon formation from biogenic gases, pollen) in coastal forest under strong solar radiation in Southern China. $PM_{2.5}$ concentration was well correlated with OC in both urban (r = 0.85, k = 5.3, p < 0.001) and rural areas (r = 0.81, k = 3, p = 0.002). This suggests that higher loading of fine particulate matter was mostly due to intensified emission of carbonaceous aerosols. CM/$PM_{2.5}$ in urban area showed better positive correlation with EC (r = 0.51, k = 4.4, p = 0.006) than with OC (r = 0.16, k = 0.3, p = 0.420), suggesting that primary emission may mostly account for particulate air pollution in urban area. CM/$PM_{2.5}$ in rural area showed considerable relationship with both OC (r = 0.61, k = 1.3, p = 0.037) and EC (r = 0.37, k = 5.3, p = 0.233). Both secondary and primary sources could be important for particulate air pollution in rural area.

Emission of Carbonaceous Aerosols from Urbanized Coastal Area

Fig. 4 shows the relationship between EC and OC for $PM_{2.5}$. During winter monsoon season, EC and OC showed good correlation (r = 0.91) for samples in urban area, but poor correlation (r = 0.59) for samples in rural area. This suggested a dominant emission source for carbonaceous aerosols and small amount of secondary organic aerosol (SOA) in urban area during winter monsoon season. The samples from urban area in summer showed very low OC/EC ratio (1.8 ± 0.9), suggesting the dominant contribution from motor vehicle emissions. Measurements of OC and EC concentrations at roadside and road tunnel showed lower OC/EC ratio (~1) than other nearby sources, such as coal combustion, residential wood burning, and forest fire (2~10, Jones and Harrison, 2005; Gelencsér *et al*., 2007; Shen *et al*., 2010). Mitigation of motor vehicle emissions may be efficient to control air pollution in summer. However, the high OC/EC ratio (4.4 ± 0.8) in winter monsoon season suggests that the high levels of carbonaceous aerosols (Fig. 2) should be contributed by multiple types of emission sources.

The large variability in OC/EC ratio in rural area indicates the combination of two or more sources of CM in rural atmosphere. The possible sources of CM in rural areas include rural emissions, carbonaceous aerosols transported from urban areas, and SOA generated from atmospheric chemistry processes (Han *et al*., 2008; Wang *et al*., 2011). OC/EC ratio was higher in rural sites (5.6 ± 5.0) than urban sites (3.6 ± 1.5), suggesting lower fraction of vehicle emissions in rural area than urban area.

Fig. 5 shows average EC and OC concentration of $PM_{2.5}$ in urban and rural areas of Xiamen (this study), in comparison with previously reported data for Beijing (Feng *et al*., 2006; Song *et al*., 2007), Guangzhou (Feng *et al*., 2006; Duan *et al*., 2007; Ding *et al*., 2011), Shanghai (Feng *et al*., 2006, 2009), Hong Kong (Duan *et al*., 2007), Europe
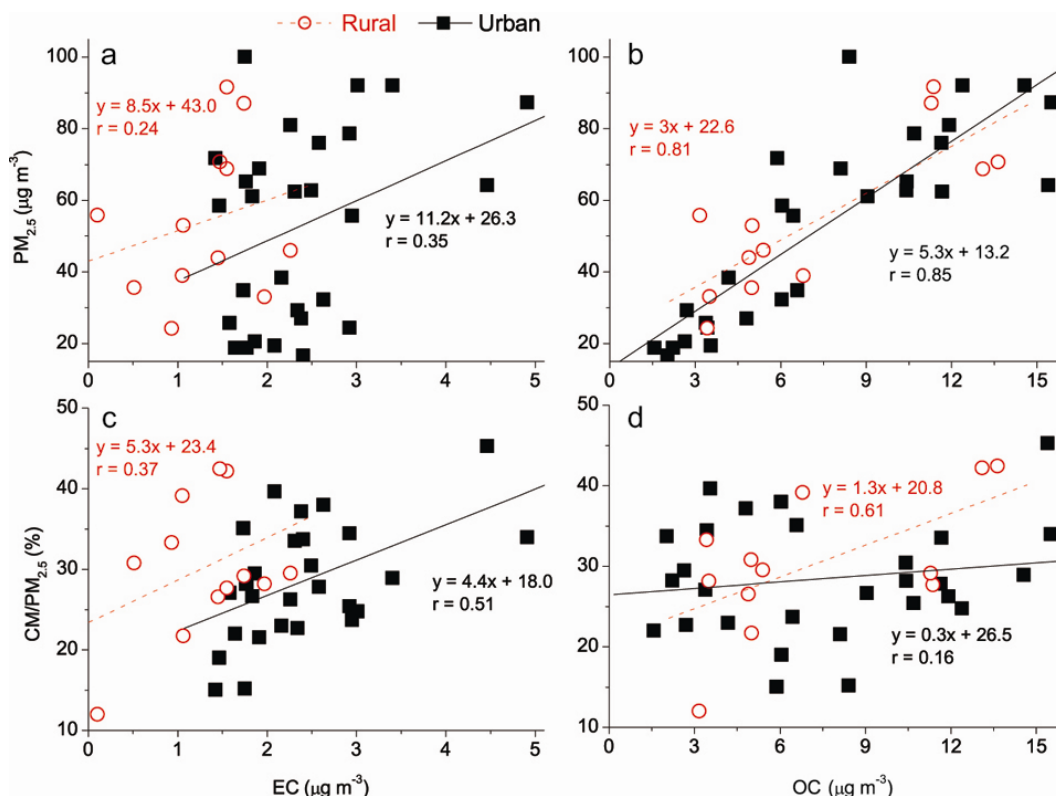

Fig. 2. Concentration of EC (a) and OC (b) in $PM_{2.5}$ in urban and rural areas of Xiamen.

Fig. 3. Relationships between EC and PM$_{2.5}$ (a), OC and PM$_{2.5}$ (b), EC and CM/PM$_{2.5}$ (c), and OC and CM/PM$_{2.5}$ (d) for samples in urban and rural areas of Xiamen.
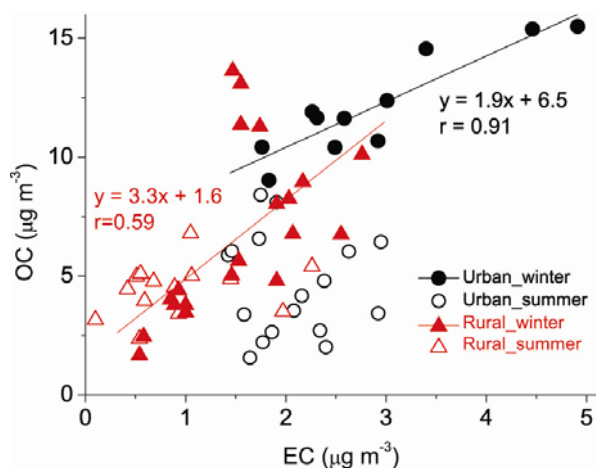

Fig. 4. Correlation between EC and OC in PM$_{2.5}$ for urban and rural samples of Xiamen.

Fig. 5. Comparison of EC and OC concentration in PM$_{2.5}$ in Xiamen (this study) with those in other cities for urban and rural areas in winter season. Average EC and OC concentrations measured by TOT method for PM$_{2.5}$ in Beijing (Feng *et al.*, 2006; Song *et al.*, 2007), Guangzhou (Feng *et al.*, 2006; Duan *et al.*, 2007; Ding *et al.*, 2011), Shanghai (Feng *et al.*, 2006, 2009), Hong Kong (Duan *et al.*, 2007), Europe (Viidanoja *et al.*, 2002; Lonati *et al.*, 2007; Viana *et al.*, 2007; Harrison and Yin, 2008), and North America (Na *et al.*, 2004; Sawant *et al.*, 2004; Park *et al.*, 2005; Grover *et al.*, 2008) are shown for comparison. Each data point in this figure represents the average value of EC or OC concentrations measured in a specific site in available literature.

(Viidanoja *et al.*, 2002; Lonati *et al.*, 2007; Viana *et al.*, 2007; Harrison and Yin, 2008), and North America (Na *et al.*, 2004; Sawant *et al.*, 2004; Park *et al.*, 2005; Grover *et al.*, 2008) in winter season. EC and OC concentrations in PM$_{2.5}$ in urban Xiamen showed higher margin value close to the concentrations in urban areas of Shanghai and Guangzhou, while lower margin value close to the concentrations in urban areas of Hong Kong. The EC and OC concentrations in the five cities in China were ranked in the following order: Beijing > Guangzhou and Shanghai > Xiamen and Hong Kong. It was noted that the similar linear distributions of
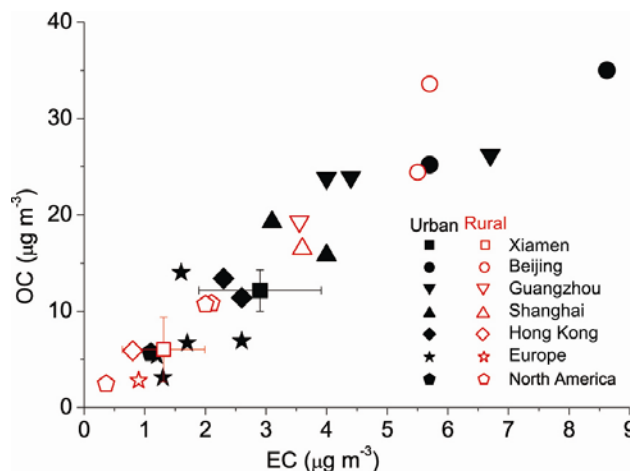
average EC-OC in China, Europe and Northern America in Fig. 5 can be probably explained by similar dominant emissions from traffic and industry sources in urban and surrounding rural areas in the three regions. Meanwhile, the EC and OC concentrations in both urban and rural areas in China were higher than those in Europe and North America. Locally emitted air pollutants may incorporate into the continental pollution plume from urbanized areas in China and transport to remote areas.

Enhanced Outflow Plume from Urban Emission

The 3-day backward trajectories during the sampling period in the rural area of Xiamen were shown in Fig. 6. Lower concentrations of EC (0.7 ± 0.3 μg/m^3) and OC (4.0 ± 1.3 μg/m^3) were observed when the air masses came from East China Sea, Japan, or South China Sea (Fig. 6(a–b)). Higher values (EC, 1.9 ± 0.4 μg/m^3; OC, 8.0 ± 3.2 μg/m^3) were observed when the air masses came from the eastern part of China (Fig. 6(c)) or urban Xiamen (Fig. 6 (d)). Intense emissions from industrial and urbanized hotspots in the eastern part of China (Beijing and surrounding urban clusters, and Shanghai and surrounding urban clusters) were highlighted in the annual EC inventory map of China (shaded area in Fig. 6(c)). The pollution of carbonaceous aerosols in the rural coastal area during winter monsoon

season was mostly associated with the transport of pollutants from emission hotspots in the eastern part of China. PM$_{2.5}$ was considerably correlated with EC concentration (r = 0.53) for the high-trajectory-group of winter monsoon season (samples of Fig. 6(c)). This may be accounted by significant vehicle and industrial emissions in a regional atmosphere in the eastern part of China (Wang *et al.*, 2011). Meanwhile, oceanic airflows occasionally made dispersion of pollutants from urban and industrial area of Xiamen to surrounding rural and coastal area during summer monsoon season. The pollution plumes transported from regional/local urbanized areas increased the concentration of carbonaceous aerosols in the rural coastal receptor area by a factor of 2–3 according to the comparison between the high- and low- trajectory-groups.

During 9–10 January 2011, the EC concentrations measured in rural Xiamen reached the highest (2.8 μg/m^3), and aerosol optical depth (AOD) were recognized hotspots (AOD > 1) in Shanghai and surrounding urban clusters (Fig. 7(a)). The high AOD (> 0.3) observed in Southern China coastal area, South China Sea and East China Sea can be justified by the AOD hotspots in Shanghai and the southward wind, which was supposed to drive the air mass from Shanghai and surrounding areas to Southern China coastal area. This is supported by the observation of high
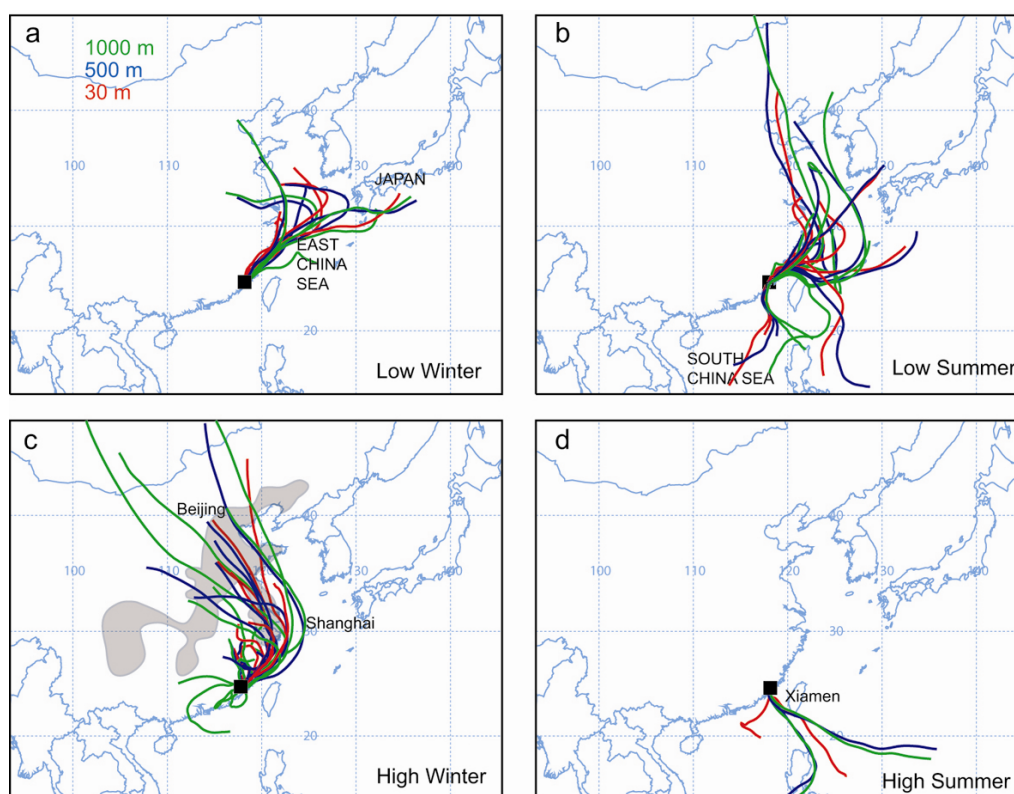

Fig. 6. Three-day backward trajectories for the samples of rural area of Xiamen. Trajectories were grouped for lower level of EC (0.7 ± 0.3 μg/m^3) and OC (4.0 ± 1.3 μg/m^3) for winter (a) and summer (b) monsoon seasons, and higher values (EC, 1.9 ± 0.4 μg/m^3; OC, 8.0 ± 3.2 μg/m^3) for winter (c) and summer (d) monsoon seasons. Backward trajectories were produced by HYSPLIT model (Draxler and Rolph 2011). Shaded area in (c) indicates high emission rate of EC (2756–10063 tone carbon per year in 1 × 1° longitude and latitude grid in the annual emission inventory map at http://www.cgrer.uiowa.edu/ EMISSION_DATA_new/) in the eastern part of China.
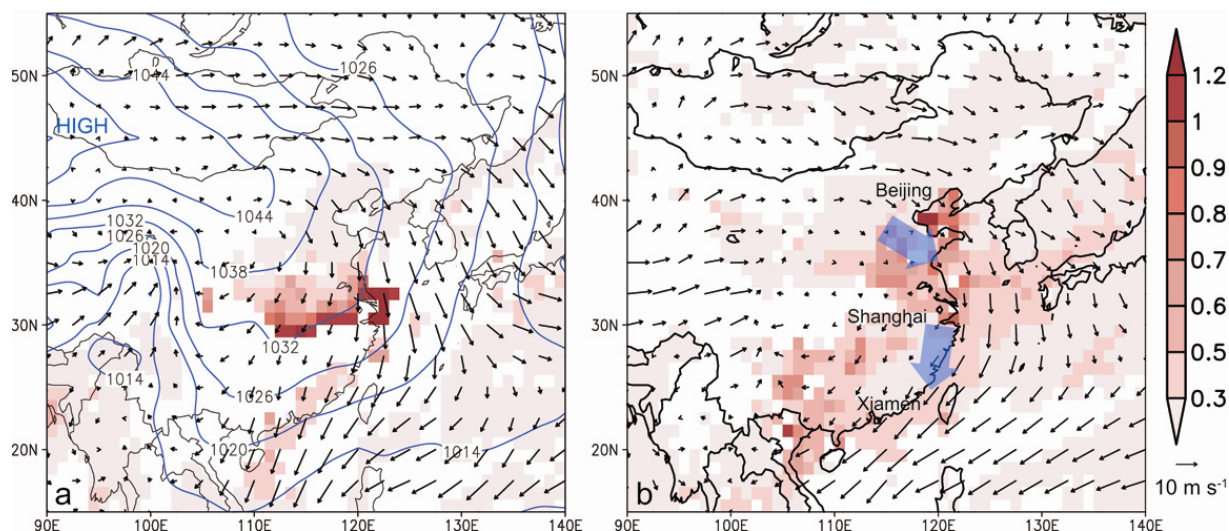
Fig. 7. (a) Map of sea level pressure (contour lines), surface wind vectors, and 550 nm AOD on 9–10 January, 2011; (b) average AOD of high-trajectory-group and wind vectors during winter monsoon season. Thick blue arrows in (b) highlight prevailing wind pathways. Meteorological data are from the NCEP reanalysis output at http://www.esrl.noaa.gov/psd/. AOD map was produced from MODIS (Moderate Resolution Imaging Spectroradiometer) data, developed and maintained by the NASA GES DISC. AOD < 0.3 generally suggests clear sky while heavy air pollution occurs for a value of AOD > 1.

EC concentrations at rural Xiamen during the 9–10 January 2011. The Mongolia high pressure system provided the driving force for the air mass traveling from the industrial and urbanized pollution hotspots in the eastern part of China to south and east. This explained the high AOD belt along coastal areas, South China Sea, and East China Sea for the high-trajectory-group (Fig. 7(b)). The average AOD map and our observation of carbonaceous aerosols intercepted at the Southern China continental edge showed significant aerosol forcing of Chinese outflow plume through the incorporation of urban emissions.

CONCLUSION

Carbonaceous aerosols emitted from urbanized coastal area not only contribute to urban air pollution, but also transport to the surrounding rural and ocean areas and significantly influence the air quality remotely. The transport of air pollutants from local and regional urbanized hotspots in the eastern part of China caused an average increase in EC concentration from 0.7 ± 0.3 to 1.9 ± 0.4 μg/m³, and an average increase in OC concentration from 4.0 ± 1.3 to 8.0 ± 3.2 μg/m³ at the rural area in Southern China continental edge. Both urban and rural areas of China showed higher concentrations of carbonaceous aerosols than those in Europe and North America, suggesting the regional dispersion of air pollution plume over Chinese continent and the surrounding region. Although much more study is necessary, the surface observation at the rural coastal receptor area, backward trajectories analysis and satellite imaging indicate 2–3 times of aerosol forcing of Chinese outflow plume by industrial and urbanized emissions. The atmospheric brown clouds over Southeastern Asia could be controlled through the effective management of anthropogenic emissions in urbanized coastal areas.

REFERENCES

Arhami, M., Kuhn, T., Fine, P.M., Delfino, R.J. and Sioutas, C. (2005). Effects of Sampling Artifacts and Operating Parameters on the Performance of a Semicontinuous Particulate Elemental Carbon/Organic Carbon Monitor. *Environ. Sci. Technol.* 40: 945–954.

Avino, P., Casciardi, S., Fanizza, C. and Manigrasso, M. (2011). Deep Investigation of Ultrafine Particles in Urban Air. *Aerosol Air Qual. Res.* 11: 654–663.

Bae, M.S., Schauer, J.J., DeMinter, J.T., Turner, J.R., Smith, D. and Cary, R.A., (2004). Validation of a Semi-continuous Instrument for Elemental Carbon and Organic Carbon Using a Thermal-optical Method. *Atmos. Environ.* 38: 2885–2893.

Bauer, J.J., Yu, X.Y., Cary, R., Laulainen, N.S. and

Berkowitz, C.M., (2009). Characterization of the Sunset Semi-Continuous Carbon Aerosol Analyzer. *J. Air Waste Manage. Assoc.* 59: 826–833.

Birch, M.E. and Cary, R.A. (1996). Elemental carbon-based Method for Occupational Monitoring of Particulate Diesel Exhaust: Methodology and Exposure Issues. *Analyst* 121: 1183–1190.

Cao, J.J., Lee, S.C., Ho, K.F., Fung, K., Chow, J.C. and Watson, J.G. (2006). Characterization of Roadside Fine Particulate Carbon and its Eight Fractions in Hong Kong. *Aerosol Air Qual. Res.* 6: 106–122.

Cao, W. and Wong, M.H. (2007). Current Status of Coastal Zone Issues and Management in China: A Review. *Environ. Int.* 33: 985–992.

Chow, J.C., Watson, J.G., Lowenthal, D.H., Chen, L.W.A. and Motallebi, N. (2010). Black and Organic Carbon Emission Inventories: Review and Application to California. *J. Air Waste Manage. Assoc.* 60: 497–507.

Chung, C.E., Ramanathan, V., Kim, D. and Podgorny, I.A., (2005). Global Anthropogenic Aerosol Direct Forcing Derived from Satellite and Ground-based Observations. *J. Geophys. Res.* 110: D24207.

Chung, S.H. and Seinfeld, J.H., (2005). Climate Response of Direct Radiative Forcing of Anthropogenic Black Carbon. *J. Geophys. Res.* 110: D11102.

Ding, X., Wang, X.M. and Zheng, M. (2011). The Influence of Temperature and Aerosol Acidity on Biogenic Secondary Organic Aerosol Tracers: Observations at a Rural Site in the Central Pearl River Delta Region, South China. *Atmos. Environ.* 45: 1303–1311

Draxler, R.R. and Rolph, G.D. (2011). HYSPLIT (HYbrid Single-Particle Lagrangian Integrated Trajectory) Model Access Via NOAA ARL READY Website (http://ready.arl.noaa.gov/HYSPLIT.php), NOAA Air Resources Laboratory, Silver Spring, MD.

Duan, J.C., Tan, J.H., Cheng, D.X., Bi, X., Deng, W., Sheng, G., Fu, J. and Wong, M.H. (2007). Sources and Characteristics of Carbonaceous Aerosol in Two Largest Cities in Pearl River Delta Region, China. *Atmos. Environ.* 41: 2895–2903.

Feng, J.L., Hu, M. Chan, C.K., Lau, P.S., Fang, M., He, L.Y. and Tang, X.Y. (2006). A Comparative Study of the Organic Matter in $PM_{2.5}$ from Three Chinese Megacities in Three Different Climatic Zones. *Atmos. Environ.* 40: 3983–3994.

Feng, Y.L., Chen, Y.J., Guo, H., Zhi, G.R., Xiong, S.C., Li, J., Sheng, G.Y. and Fu, J.M. (2009). Characteristics of Organic and Elemental Carbon in $PM_{2.5}$ Samples in Shanghai, China. *Atmos. Res.* 92: 434–442.

Gelencsér, A., May, B., Simpson, D., Sánchez-Ochoa, A., Kasper-Giebl, A., Puxbaum, H., Caseiro, A., Pio, C. and Legrand, M. (2007). Source Apportionment of $PM_{2.5}$ Organic Aerosol over Europe: Primary/Secondary, Natural/Anthropogenic, and Fossil/Biogenic Origin. *J. Geophys. Res.* 112: D23S04.

Grover, B.D., Eatough, N.L., Woolwine, W.R., Cannon, J.P., Eatough, D.J. and Long, R.W. (2008). Semi-continuous Mass Closure of the Major Components of Fine Particulate Matter in Riverside, CA. *Atmos. Environ.* 42: 250–260.

Gu, J., Bai, Z., Liu, A., Wu, L., Xie, Y., Li, W., Dong, H. and Zhang, X. (2010). Characterization of Atmospheric Organic Carbon and Element Carbon of $PM_{2.5}$ and PM_{10} at Tianjin, China. *Aerosol Air Qual. Res.* 10: 167–176.

Han, Y.M., Cao, J.J., Chow, J.C., Watson, J.G., An, Z.S. and Liu, S.X. (2008). Distribution and Origin of Carbonaceous Aerosol over a Rural High-mountain Lake Area, Northern China and its Transport Significance. *Atmos. Environ.* 42: 2405–2414.

Harrison, R.M. and Yin, J.X. (2008). Sources and Processes Affecting Carbonaceous Aerosol in Central England. *Atmos. Environ.* 42: 1413–1423.

Ho, K. F., Lee, S.C., Cao, J.J., Chow, J.C., Watson, J.G. and Fung, K. (2006). Variability of Levels, Water Soluble and Isotopic Composition of Organic and Elemental Carbon in Hong Kong Urban Atmosphere. *Atmos. Chem. Phys.* 6: 1–8.

Jeong, C.H., Hopke, P.K., Kim, E. and Lee, D.W. (2004). The Comparison between Thermal-optical Transmittance Elemental Carbon and Aethalometer Black Carbon Measured at Multiple Monitoring Sites. *Atmos. Environ.* 38: 5193–5204

Jones, A.M. and Harrison, R.M. (2005). Interpretation of Particulate Elemental and Organic Carbon Concentrations at Rural, Urban and Kerbside Sites. *Atmos. Environ.* 39: 7114–7126.

Kim, K., Sekiguchi, K., Kudo, S. and Sakamoto, K. (2011). Characteristics of Atmospheric Elemental Carbon (Char and Soot) in Ultrafine and Fine Particles in a Roadside Environment, Japan. *Aerosol Air Qual. Res.* 11: 1–12.

Lim, H.J., Turpin, B.J., Edgerton, E., Hering, S.V., Allen, G., Maring, H., Solomon, P., (2003). Semicontinuous Aerosol Carbon Measurements: Comparison of Atlanta Supersite Measurements. *J. Geophys. Res.* 108: 8419.

Liu, H., Jacob, D.J., Bey, I., Yantosca, R.M., Duncan, B.N. and Sachse, G.W. (2003). Transport Pathways for Asian Pollution Outflow over the Pacific: Interannual and Seasonal Variations. *J. Geophys. Res.* 108: 8786.

Lonati, G., Ozgen, S. and Giugliano, M. (2007). Primary and Secondary Carbonaceous Species in $PM_{2.5}$ samples in Milan (Italy). *Atmos. Environ.* 41: 4599–4610.

Menon, S., Hansen, J., Nazarenko, L. and Luo, Y. (2002). Climate Effects of Black Carbon Aerosols in China and India. *Science* 297: 2250–2253.

Na, K., Sawant, A.A., Song, C. and Cocker III, D.R. (2004). Primary and Secondary Carbonaceous Species in the Atmosphere of Western Riverside County, California. *Atmos. Environ.* 38: 1345–1355.

NIOSH (1999). Elemental Carbon (Diesel Particulate): Method 5040., in: O'Connor., M.E.c.a.P.F. (Ed.), NIOSH Manual of Analytical Methods, National Institute of Occupational Safety and Health, U.S. Department of Health and Human Services, Cincinnati, OHh.

Nunes, T.V. and Pio, C.A. (1993). Carbonaceous Aerosols in Industrial and Coastal Atmospheres. *Atmos. Environ.* 27: 1339–1346.

Pöschl, U. (2005). Atmospheric Aerosols: Composition, Transformation, Climate and Health Effects. *Angew. Chem. Int. Ed.* 44: 7520–7540.

Ramanathan, V. and Carmichael G. (2008). Global and Regional Climate Changes Due to Black Carbon. *Nat. Geosci.* 1: 221–227.

Rice, J. (2004). Comparison of Integrated Filter and Automated Carbon Aerosol Measurements at Research Triangle Park, North Carolina. *Aerosol Sci. Technol.* 38: 23–36.

Sawant, A.A., Na, K., Zhu, X.N. and Cocker III, D.R. (2004). Chemical Characterization of Outdoor $PM_{2.5}$ and Gas-phase Compounds in Mira Loma, California. *Atmos. Environ.* 38: 5517–5528.

Shen, Z., Han, Y., Cao, J., Tian, J., Zhu, C., Liu, S., Liu, P. and Wang, Y. (2010). Characteristics of Traffic- related Emissions: A Case Study in Roadside Ambient Air over Xi'an, China. *Aerosol Air Qual. Res.* 10: 292–300.

Shi, J, Peng, Y., Li, W., Qiu, W., Bai, Z., Kong, S. and Jin, T. (2010). Characterization and Source Identification of PM10-bound Polycyclic Aromatic Hydrocarbons in Urban Air of Tianjin, China. *Aerosol Air Qual. Res.* 10: 507-518

Song, Y., Tang, X.Y., Xie, S.D., Zhang, Y.H., Wei, Y.J., Zhang, M.S., Zeng, L.M. and Lu, S.H. (2007). Source Apportionment of $PM_{2.5}$ in Beijing in 2004. *J. Hazard. Mater.* 146: 124–130.

Turpin, B.J. and Lim, H.J. (2001). Species Contributions to $PM_{2.5}$ Mass Concentrations: Revisting Common Assumptions for Estimating Organic Mass. *Aerosol Sci. Technol.* 35: 602– 610.

UNEP and WMO (2011). Integrated Assessment of BC and Tropospheric Ozone.

Viana, M., Maenhaut, W., ten Brink, H. M., Chi, X., Weijers, E., Querol, X., Alastuey, A., Mikuska, P. and Vecera, Z. (2007). Comparative Analysis of Organic and Elemental Carbon Concentrations in Carbonaceous Aerosols in Three European Cities. *Atmos. Environ.* 41: 5972–5983.

Viidanoja, J., Sillanpaa, M., Laakia, J., Kerminen, V.M., Hillamo, R., Aarnio, P. and Koskentalo, T. (2002). Organic and Black Carbon in $PM_{2.5}$ and PM_{10}: 1 Year of Data from an Urban Site in Helsinki, Finland. *Atmos. Environ.* 36, 3183–3193.

Wang, G., Li, J., Cheng, C., Hu, S., Xie, M., Gao, S., Zhou, B., Dai, W., Cao, J. and An, Z. (2011). Observation of Atmospheric Aerosols at Mt. Hua and Mt. Tai in Central and East China during Spring 2009-Part 1: EC, OC and Inorganic Ions. *Atmos. Chem. Phys.* 11: 4221–4235.

Xiao, Z., Zhang, Y., Hong, S., Bi, X., Jiao, L., Feng, Y. and Wang, Y. (2011). Estimation of the Main Factors Influencing Haze, Based on a Long-term Monitoring Campaign in Hangzhou, China. *Aerosol Air Qual. Res.* 11: 873–882.

Xu, B., Cao, J., Hansen, J., Yao, T., Joswia, D.R., Wang, N., Wu, G., Wang, M., Zhao, H., Yang, W., Liu, X. and He, J. (2009). Black Soot and the Survival of Tibetan Glaciers. *Proc. Nat. Acad. Sci. U.S.A.* 106: 22114–22118.

Yang, H. and Yu, J.Z., (2002). Uncertainties in Charring Correction in the Analysis of Elemental and Organic Carbon in Atmospheric Particles by Thermal/Optical Methods. *Environ. Sci. Technol.* 36: 5199–5204.

Zhang, Q., Streets, D. G., Carmichael, G. R., He, K., Huo, H., Kannari, A., Klimont, Z., Park, I., Reddy, S., Fu, J. S., Chen, D., Duan, L., Lei, Y., Wang, L. and Yao, Z. (2009a). Asian Emissions in 2006 for the NASA INTEX-B Mission. *Atmos. Chem. Phys.* 9: 5131–5153.

Zhang, R., Ho, K.F., Cao, J., Han, Z., Zhang, M., Cheng, Y. and Lee, S.C. (2009b). Organic Carbon and Elemental Carbon Associated with PM_{10} in Beijing during Spring Time. *J. Hazard. Mater.* 172: 970–977.